

Effects of SOPC on the Phase Behaviors of the DSPC/DOPC/Cholesterol Biomembrane Model System

Fanrong Kong

Laboratory of Prof. Gerald Feigenson

Department of Molecular Biology and Genetics

Cornell University, Ithaca, New York 14853 USA

KEYWORDS

lipid, phase diagram, fluorescence microscopy, GUV, electroswellling, photo-induction.

FOOTNOTES

Abbreviations and symbols: DSPC, 1,2-distearoyl-sn-glycero-3-phosphatidylcholine; DOPC, 1,2-dioleoyl -sn-glycero-3-phosphatidylcholine; Chol, cholesterol; POPC, 1-palmitoyl-2-oleoyl-sn-glycero-3-phosphatidylcholine; SOPC, 1-stearoyl-2-oleoyl-sn-glycero-3-phosphatidylcholine; 18:0-18:2 PC, 1-stearoyl-2-linoleoyl-sn-glycero-3-phosphatidylcholine; 18:0-22:6 PC, 1-stearoyl-2-docosahexaenoyl-sn-

glycero-3-phosphatidylcholine; C12:0-DiI, 1,1'-didodecanyl-3,3,3',3'-tetramethylindocarbocyanine perchlorate; C20:0-DiI, 1,1'-dieicosanyl-3,3,3',3'-tetramethylindocarbocyanine perchlorate; GUV, Giant Unilamellar Vesicle, $L\alpha$, liquid disordered phase; L_o , liquid ordered phase; $L\beta$, solid/gel phase; $L\beta'$, tilted solid/gel phase.

ABSTRACT

The phase diagram of the DSPC/DOPC/cholesterol biomembrane model system was recently determined by studies in our laboratory. However, the component DOPC does not occur in animal cell plasma membranes, but was chosen for convenience in solving the phase diagram. In my study, DOPC was replaced stepwise by the naturally-occurring SOPC to determine its effect on the high cholesterol boundary of the $L\alpha$ + L_o two-phase region. Giant unilamellar vesicles with the chosen compositions, probed with the fluorescent dye C12:0-DiI, were made by electrosweeling and their phase behaviors were examined by fluorescence microscopy. From 0 to 45% replacement of DOPC by SOPC, the middle part of the boundary shifts only a small amount, from cholesterol mole fraction 0.38 down to mole fraction 0.30 – 0.35. The $L\alpha$ side of the boundary remains essentially unchanged. Above 50% replacement, photo-induced artifacts obscure the real phase behavior at the middle part of the boundary, but might represent the actual boundary termination. Above 70% replacement of DOPC by SOPC, no phase-separation was observed for the $L\alpha$ side of the boundary. The size and shape of the $L\alpha$ + L_o two-phase region can be related to the structures of the lipids.

INTRODUCTION

By the fluid mosaic model (1), the lipids in the plasma membrane were modeled as a homogenous fluid bilayer. However, in the 30 years since that simple model, studies of phase behaviors of biomembranes emphasize the non-random mixing of lipids and address some fundamental and challenging questions in biology. The phases observed in chemically simple lipid bilayer mixtures are very intriguing phenomena that are closely related to the lipid raft concept. Lipid rafts are described as distinct domains in biomembranes, rich in sphingolipids, cholesterol, and associated with selected proteins (2, 3). Lipid rafts are suspected of playing important roles in many cellular functions, including lipid and protein localization (2-4), viral and bacterial infection, membrane fission and fusion (5), and signal transduction pathways across the membrane (2, 3).

A comprehensive phase diagram for the 3-component DSPC/DOPC/chol model system (Figure 1) shows rich phase behaviors (6). While this mixture of PCs and cholesterol serves as a chemically simplified model for the outer leaflet of animal cell plasma membrane (7), both DOPC and DSPC are not abundant in real biomembranes. Instead, these lipids are chosen for our studies because their phase boundaries are clear. In addition, lack of polyunsaturation makes these lipids relatively more stable and easier to handle. Despite this drawback, by the introduction of a fourth component, this well established system can serve as a powerful platform to study the phase behaviors and interactions of many other biologically more important lipids. Therefore, our laboratory is studying components that are actually found in real biomembranes, including POPC, lipids with polyunsaturated acyl chains, sphingomyelin, and small peptides.

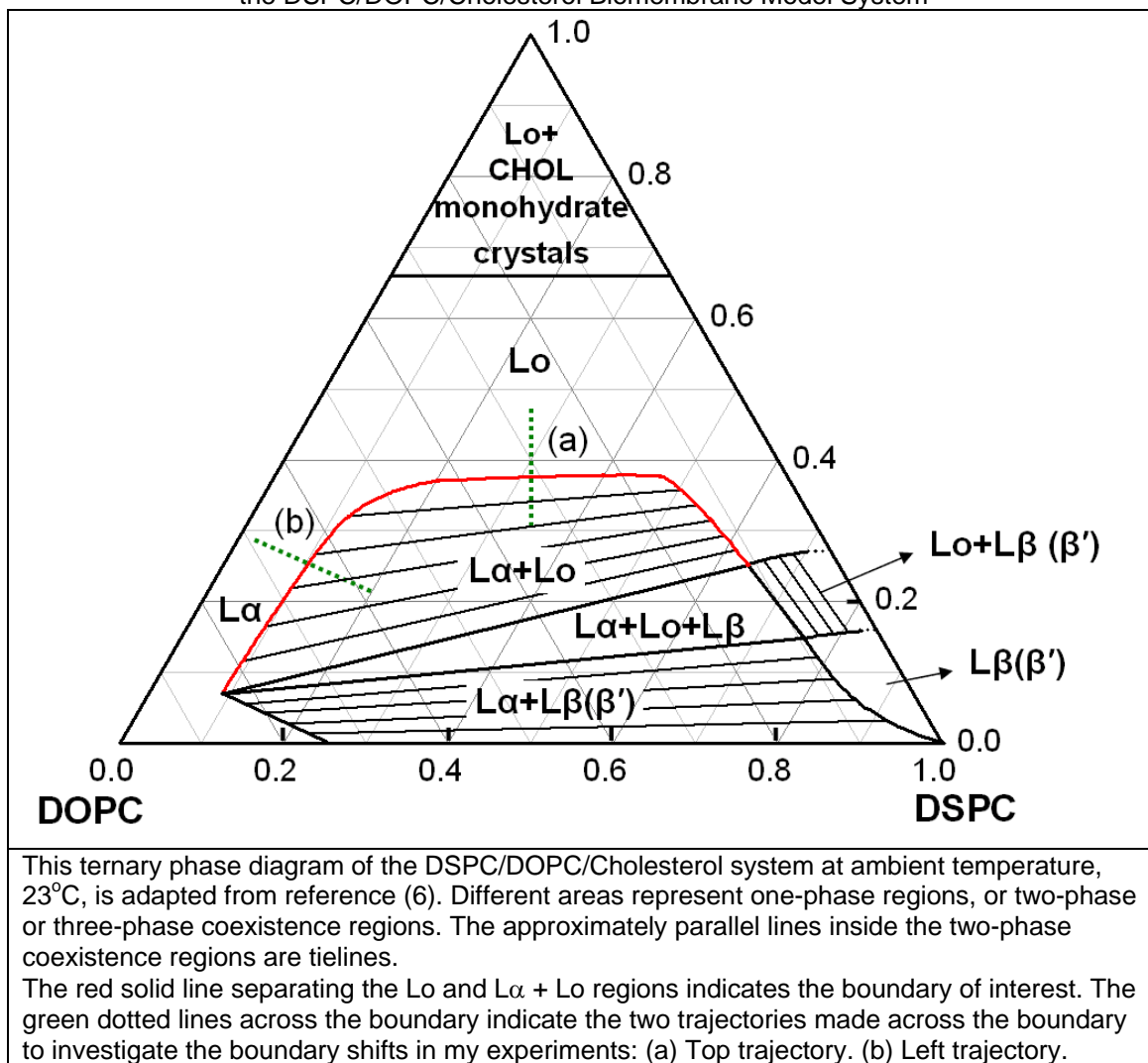
Various fluid PCs having one 18-carbon saturated acyl chain, and one chain that is an ω -3 or ω -6 polyunsaturated fatty acid are actually found in real biomembranes. ω -3 and ω -6 fatty acids are of great interest because of their relevance to human health (8). In order to examine these lipids systematically, a comprehensive study of a series of lipids with increasing number of double bonds can be proposed: SOPC (18:0-18:1, with a ω -9 acyl chain), 18:0-18:2 PC (with a ω -6 acyl chain), and 18:0-22:6 PC (with a ω -3 (DHA) acyl chain), each of these as the fourth component, to be introduced into the DSPC/DOPC/chol system.

In this report, I focus only on SOPC; 18:0-18:2 PC and 18:0-22:6 PC will be examined by other researchers in our group after the effects of SOPC have been determined. I started with SOPC because it is the chemically simplest and most stable among the series. Stepwise introduction of SOPC was expected to produce interpretable changes to the phase diagram, and retain the overall architecture of the phase diagram determined for DSPC/DOPC/chol.

In the phase diagram of DSPC/DOPC/chol, one of the most important and most accurately determined boundaries is the high cholesterol boundary of the liquid disordered ($L\alpha$) and liquid ordered (Lo) two-phase coexistence region, which separates this two-phase region from the one-phase $L\alpha$ or Lo region (Figure 1). The goal of my project was to determine the direction and extent of the movement of this boundary as DOPC was replaced by SOPC. Ultimately, with much more data, a tetrahedral phase diagram will be constructed to view the contour of the boundaries in three dimensions.

Phosphate assay for measuring phospholipids concentration in stock solutions, the electrosweeling method for preparing GUV, and fluorescence microscopy were the major experimental methods I used.

Figure 1 The Ternary Phase diagram of the DSPC/DOPC/Cholesterol Biomembrane Model System



MATERIALS AND METHODS

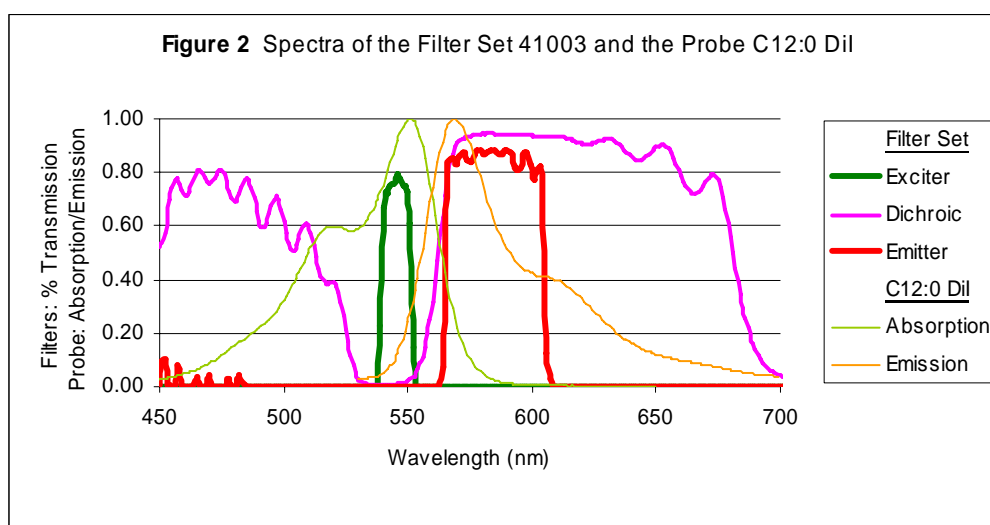
Materials

Phospholipids (DOPC, DSPC, SOPC) were obtained from Avanti Polar Lipids, Inc. (Alabaster, Alabama) in chloroform solutions, and further diluted as stock solutions. Using an HP 8452A spectrophotometer from Hewlett-Packard (Palo Alto, California), the concentrations of the phospholipids were determined by phosphate assay (9), an accurate and safe quantitative spectrophotometric assay for concentrations of phospholipids. Cholesterol was obtained from Nu-Check Prep, Inc. (Elysian, Minnesota) in powder form, and was made into stock solutions in chloroform by standard gravimetric procedures.

The fluorescent dye used in this experiment, C12:0-DiI, was obtained from Molecular Probes of Invitrogen Corp. (Carlsbad, California) and was made into stock solution in ethanol. Its absorption and emission spectra are in Figure 2 (data from Invitrogen). The concentration of the fluorescent dye was assayed spectrophotometrically and calculated using its extinction coefficient provided by Molecular Probes. For a region of two-phase coexistence, dyes that partition differently into each phase would produce complementary images of the GUVs. Yet ideally, one dye that partitions clearly into either phase would be sufficient to detect the phase behaviors. C12:0-DiI partitions into the $L\alpha$ phase (G. W. Feigenson, unpublished data) and was adequate for this experiment. In order to minimize the perturbation by the dye of the phase behavior of the lipids, I used only it at a relatively low dye to lipid ratio of 1:1000 in the GUV samples.

The fluorescence microscope used was a Nikon (Japan) Diaphot-TMD inverted fluorescence microscope equipped with a 100W short-arc mercury lamp from Osram

(Germany). A 100X oil immersion objective was used. The filter set 41003 from Chroma Technology Corp. (Rockingham, Vermont) included the exciter HQ546/12x, the dichroic mirror Q560LP, and emitter HQ585/40m. The spectral transmissions of the filters are in Figure 2 (data from Chroma). This filter set was specifically designed for DiI: the spectrum of the exciter matches the absorption peak of DiI and the spectra of the dichroic mirror and emitter match the emission peak (Figure 2). All the GUV images in this report are taken with a Sensys CCD camera from Photometrics (Tucson, Arizona)



This chart shows the spectra of the components in the filter set, and the fluorescent dye C12:0-DiI. The spectrum of the exciter matches the absorption peak of DiI and the spectra of the dichroic mirror and emitter match the emission peak, as a design to maximize efficiency.
(Data from Chroma and Invitrogen.)

Methods

To investigate the targeted boundary, two trajectories were made across the boundary: one across the top part of the boundary, close to the location of the critical point, with a fixed ratio of DOPC:DSPC = 1:1, and varying cholesterol percentages; the other one across the boundary on the left, with a fixed ratio of cholesterol to DOPC = 7:3

and varying DSPC percentages (Figure 1). A series of GUV samples was prepared along the trajectory. Samples without SOPC were prepared and examined before starting the actual investigations, in order to practice the experimental techniques and reproduce the results of previous studies. Next, for each DOPC concentration in the original DSPC/DOPC/chol mixture, DOPC was replaced stepwise by SOPC, keeping the total (DOPC + SOPC) equal to that of the DOPC alone in the original DSPC/DOPC/chol mixture.

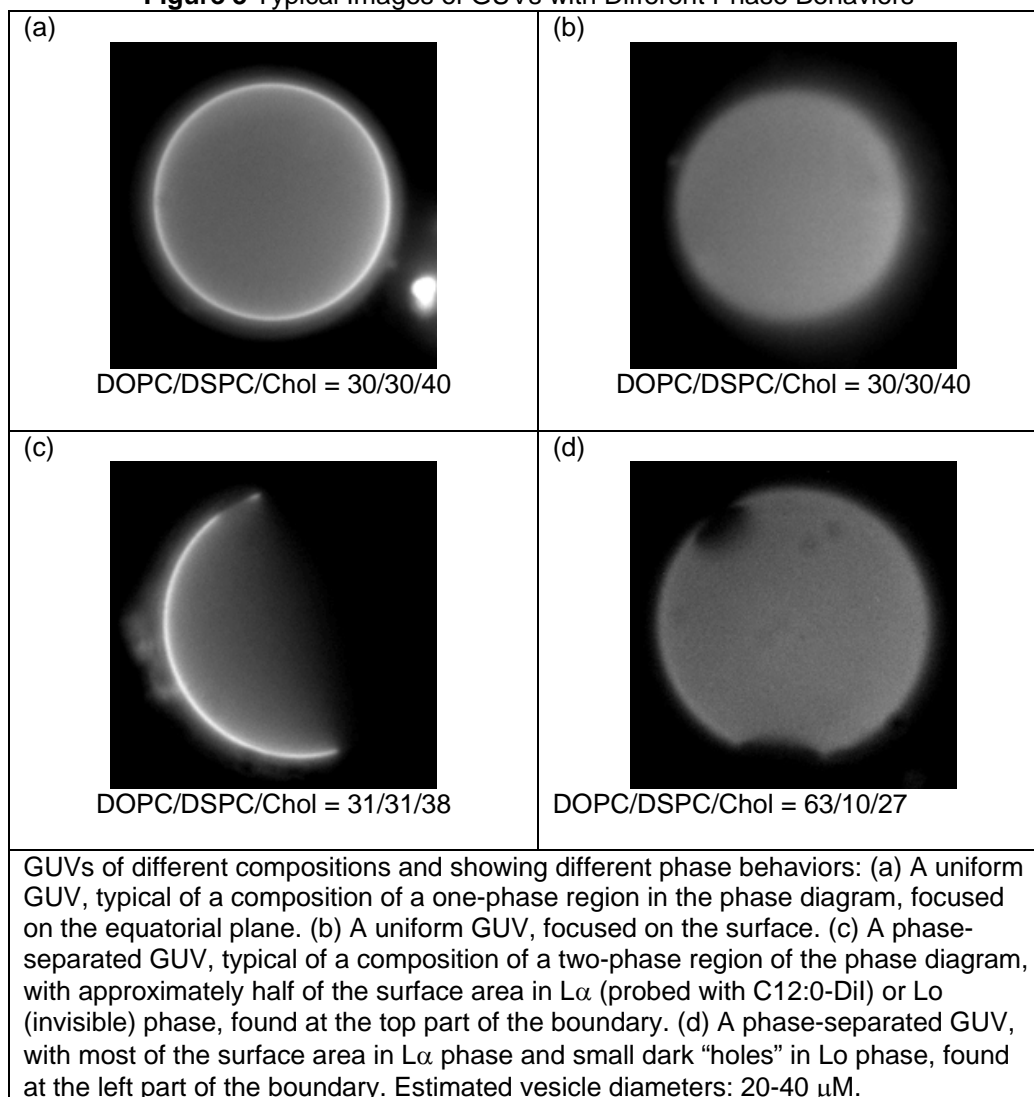
The GUV samples were prepared by electroswellling (10, 11), as follows: Using a gastight 50 μ L syringe with a PB600-1 repeating dispenser with a 0.5 μ L minimal volume from Hamilton Company (Reno, Nevada), the lipids and dye were measured, then mixed and spread on Indium-Tin Oxide (ITO)-coated glass slides, obtained from Delta Technologies (Stillwater, Minnesota), while being heated at 65 $^{\circ}$ C, then pumped under vacuum at 30-50 mtorr for 1-2 hr. Rubber o-rings were used to create a chamber for hydrating this lipid film, and 100mM aqueous sucrose solution added. The lipid samples in these chambers were heated at 70 $^{\circ}$ C while applying a 1-volt sine wave at 5 Hz for 2 hours. The samples were slowly cooled in Styrofoam boxes overnight to ambient temperature, about 23 $^{\circ}$ C and collected and viewed at the same temperature.

When each GUV sample was examined, the yield of GUVs produced in each sample was noted because low yields can indicate faulty sample preparation. Also, at least a moderate yield was required to prevent errors due to small numbers of observations. At least two slides of each sample composition were examined, and the number vesicles viewed was on the order of hundreds. The samples were distinguished by their different phase behaviors and characterized into two categories: 1) uniform,

when the dye was homogenously distributed throughout the whole GUV; or 2) phase-separated, when the dye was localized only in parts of the GUV (Figure 3). The phase boundary was marked as the midpoint between the composition that showed phase separation and the closest examined composition that appeared uniform. The direction and extent of phase boundary change thereby could be determined.

The diameters of all GUVs observed were estimated to be 20-40 μM by other experiments. This estimation applies to Figure 3, 5, and 6.

Figure 3 Typical Images of GUVs with Different Phase Behaviors

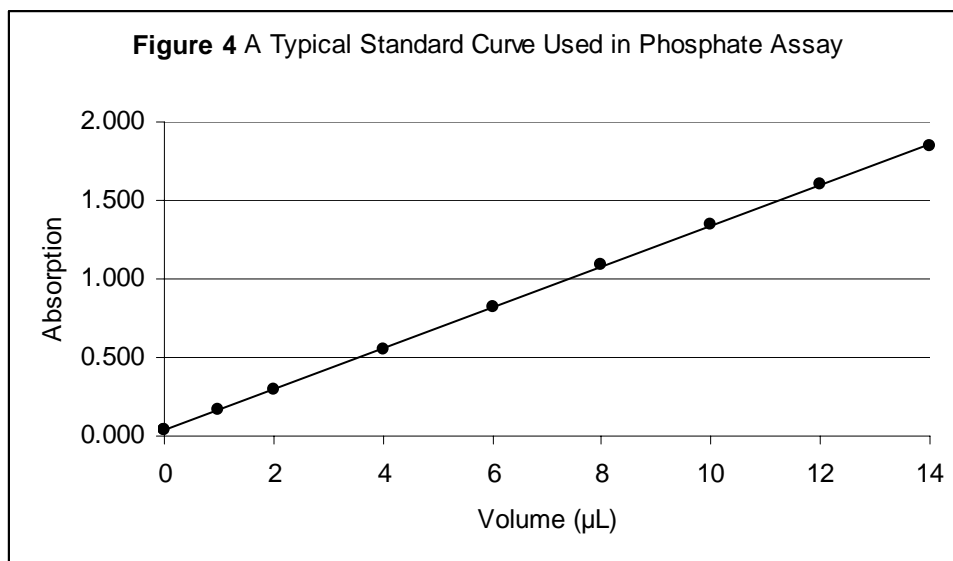


The author was trained by the members of the Feigenson Laboratory, but performed all the experimental techniques independently throughout the whole project, including phosphate assays, GUV preparation, fluorescence microscopy, and data analysis.

RESULTS

Phosphate Assay

The concentration of the standard inorganic phosphate used was 5.265 mM. By comparing the absorption of the phospholipids and the standard curve of the standard inorganic phosphate (Figure 4), the concentrations of the phospholipids can be calculated.



In phosphate assay, a standard curve of the standard inorganic phosphate was created on each day of experiment by measuring the absorptions of the standard inorganic phosphate of different concentrations. Absorptions of phospholipid stock solutions are compared to the standard curve to obtain their concentrations.

The concentrations of the phospholipid stocks were measured assayed every few months throughout the period of the experiment. Concentrations remained stable over several months. The concentrations of the lipids used in the experiment are in Table 1.

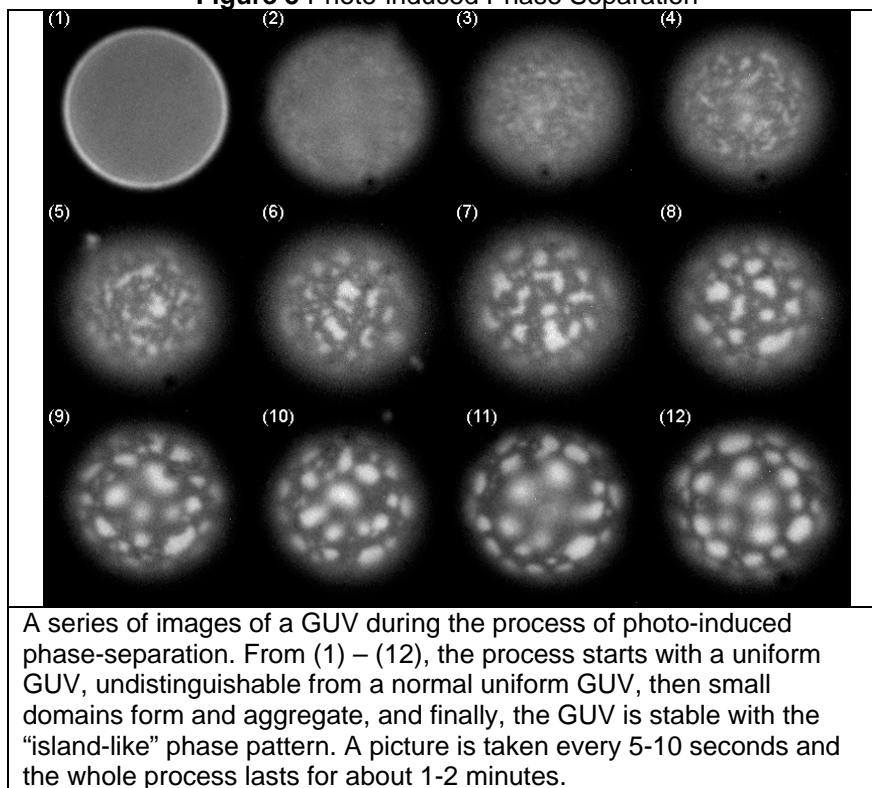
Table 1 Concentrations of the Lipids and Dyes Used

Lipid	DOPC	SOPC	DSPC	Cholesterol	C12:0-Dil
Conc. (mM)	19.5	10.1	13.0	15.0	0.10

GUV Results

The GUV appearance from one sample typically showed one characteristic phase behavior. When more than one kind of phase behavior was observed in one sample, the exact fractions of each kind of GUVs were not recorded. However, the phase behavior, i.e., one phase or two, was decided visually by the majority of the GUVs observed. No samples showed non-definitive behaviors, i.e. having approximately equal numbers of two kinds of GUVs.

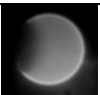
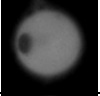
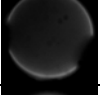
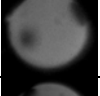
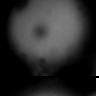
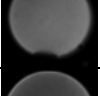
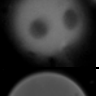
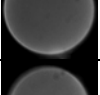
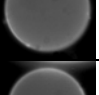
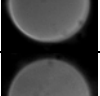
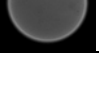
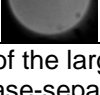
Four major categories of GUV appearances were actually observed: uniform (Figure 3 (a), (b)); “half-and-half” phase-separated (Figure 3 (c)); “small holes” phase-separated (Figure 3 (d)); and “photo-induced” separated (Figure 5). While the first three kinds of phase behaviors are stable during the time of observation, photo-induction was a dynamic process in which GUVs change their appearance from uniform to “island-like” phase-separated. The process did not start during the many hours of sample equilibration in the dark, but instead only after the GUVs were exposed to light in the viewable field of the microscope.

Figure 5 Photo-induced Phase Separation

GUV images are the raw data of the experiment. Because of the limitation of space, only selected images of GUV samples are shown in Figure 6, in order to illustrate the method of data collection and organization. The complete data of GUV phase behaviors along with the corresponding compositions are tabulated in Appendix A, and plotted in Figure 7. Compositions were chosen in order to trace the position of the boundary along a specific path ("trajectory") as shown in Figure 1.

Figure 6 Images of Selected GUV Samples

(a) Left Trajectory

Replacement SOPC	0%	10%
17.4%		
15.8%		
14.1%		
12.3%		
10.5%		
8.5%		
6.5%		
4.5%		
Note the difference of the larger dark areas, indicating phase-separation (10.5% SOPC and above) and the smaller dots scattered around in all images, which are just artificial speckles from the microscope.		

(b) Top Trajectory

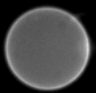
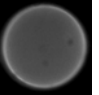
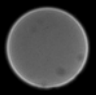
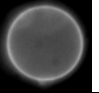
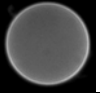
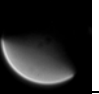
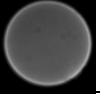
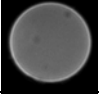
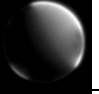
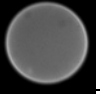
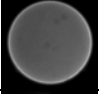
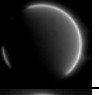
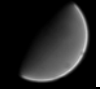
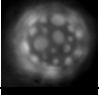
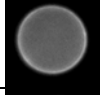
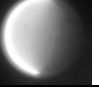

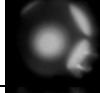
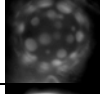
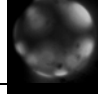

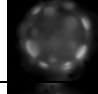
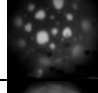
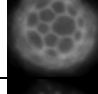
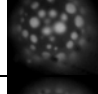
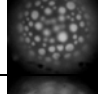
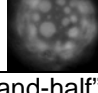
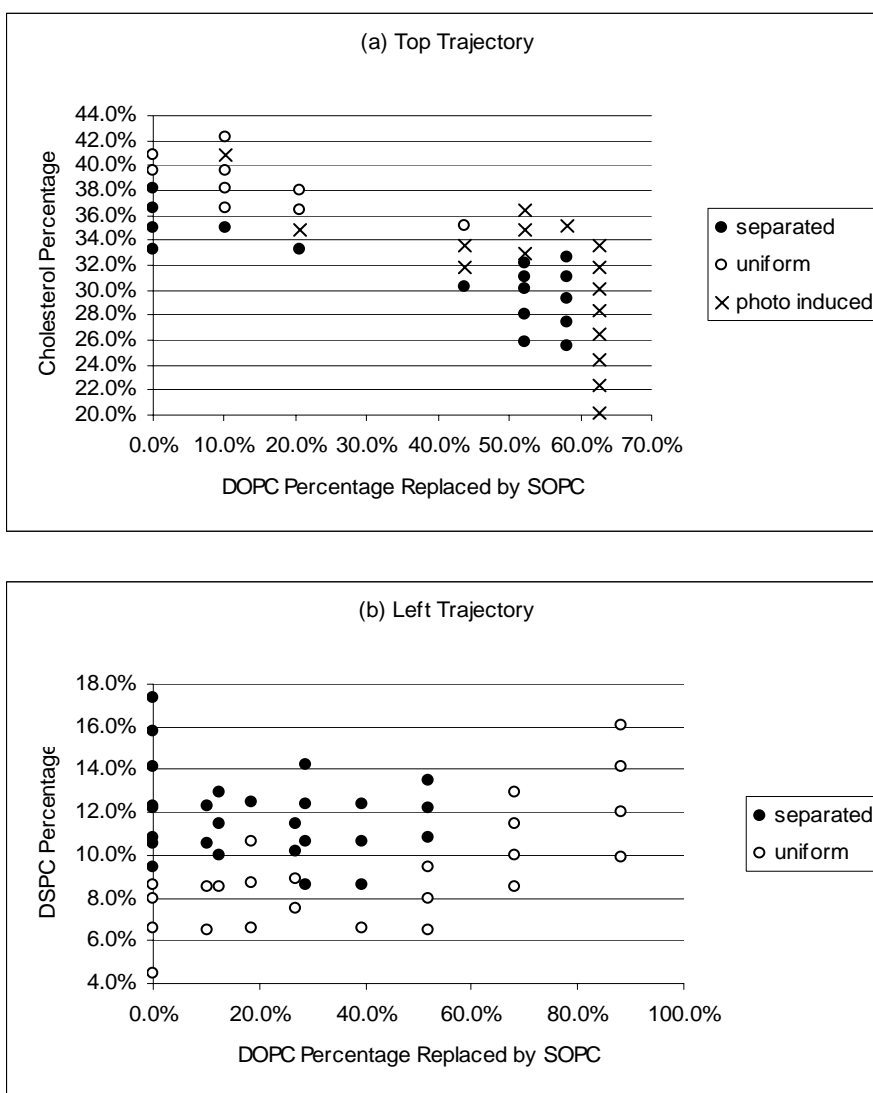
Replacement Chol	0%	10%	21%	43%	62%
42.2%					
41%					
39.5%					
38%					
36.5%					
35%					
33.5%					
32%					
30%					
28.3%					
26.4%					
24.4%					
22.3%					
20.1%					
Note the difference of real phase-separation, indicated by “half-and-half” separated GUVs, and photo-induced separation, indicated by GUVs showing island-like” phase pattern.					

Figure 7 Effect of SOPC on the
DSPC/DOPC/Cholesterol Phase Diagram



Along each vertical series, the phase boundary positions were judged to be between the two closet points with separated and uniform GUVs. The charts in whole show the shift of boundary positions as SOPC replacement increased along the horizontal axis.

DISCUSSION

The Shift of the Boundary

As shown in Figure 7a for the top trajectory, replacement of less than 45% of the DOPC by SOPC shifts the middle part of the boundary to a lower cholesterol concentration gradually, shrinking the two-phase boundary from cholesterol concentration of 39% to between 30% – 35%. However, above 50% replacement, photo-induced domain formation obscures the real phase behavior at the middle part of the boundary. Because the original state of the GUVs was uniform, it is reasonable to group the photo-induced behavior together with the uniform category. In this way of analysis, from 58% to 62% replacement, the two-phase region disappears rather abruptly, over a tiny range of SOPC replacement. An abrupt shift of phase boundary is intriguing. However, at this time it is not known whether this treatment of the photo-induced effects is the correct method of analysis, and further study is demanded for this part of the boundary.

As shown in Figure 7b for the left trajectory, with replacement of up to 50% of the DOPC by SOPC, the position of the boundary remains almost unchanged within experimental uncertainty. With replacement above 70%, no phase-separation was observed, at least to 15% DSPC. Therefore, for SOPC replacement of DOPC above 70%, either the left side of the boundary is located at higher than 15% DSPC, or else there was no separation at all. This boundary shift should therefore also be studied further, particularly for the region between 50% and 70% replacement to find out how abruptness the boundary shifts, and for higher DSPC percentage to find out how much the boundary really shifts. However, I note that an abrupt disappearance of $L\alpha + L_o$ phase coexistence

at about 60% replacement of DOPC by SOPC, found for the middle part of the boundary, is consistent with my observations of this left side boundary.

The photo-induced domain phenomenon complicated the otherwise straightforward analysis of the results. Although the details of the nature of this phenomenon are not understood, it seemed to happen more often at the compositions near the boundary and at higher percentages of replacement of DOPC by DSPC. Also, photo-induced domains were only observed at the top trajectory, but not the left trajectory. Each sample had been equilibrated at ambient temperature, in the dark, for 15 - 20 hours, but the photo-induced domains did not appear until the GUVs were exposed to intense light source in the viewable field of the microscope.

Error Analysis

The error in the concentration of phospholipid stock solutions, given by the standard deviations of the samples in phosphate assay, was less than 2%. The error in the concentration of cholesterol stock solution fresh made by the standard gravimetric procedures was less than 1%. However, while phosphate assay was performed to check the concentrations of the phospholipid stocks, there was no simple way to assure the accuracy of the concentration of the cholesterol stock throughout the period of the experiment. By careful handling of the cholesterol stock, it was assumed that no chemical degradation occurred to the solution and the concentration remained the same. The error contributed by the gastight syringe and the repeating dispenser, was less than 1%.

Because of the relatively high accuracy in the experimental techniques, the error in the boundary positions was limited largely by the increments of the cholesterol

concentration for the top trajectory, and DSPC concentrations for the left trajectory, which were about 2% in concentration.

The Choice of Dyes

For a region of two-phase coexistence, in principle, one dye that partitions clearly into either phase was enough to detect the phase behaviors. There is no problem for the trajectories approximately perpendicular to the tielines (such as the top trajectory in Figure 1), because there are substantial areas of each phase in phase-separation so that the detection is easy. However, for the trajectories approximately parallel to the tielines (such as the left trajectory in Figure 1), as the trajectory goes from the one-phase region to the two-phase region, GUVs are expected to change from being uniform to having a new phase that takes up only a tiny surface area. The accuracy of the boundary position depends on the sensitive detection of the small area of one phase embedded in an otherwise uniform surface. Therefore, a dye that partitions into the smaller phase, instead of a dye that partitions into the larger phase, would be more helpful because it is easier to detect very small bright dots on the surface of GUVs under the microscope, instead of very small dark holes.

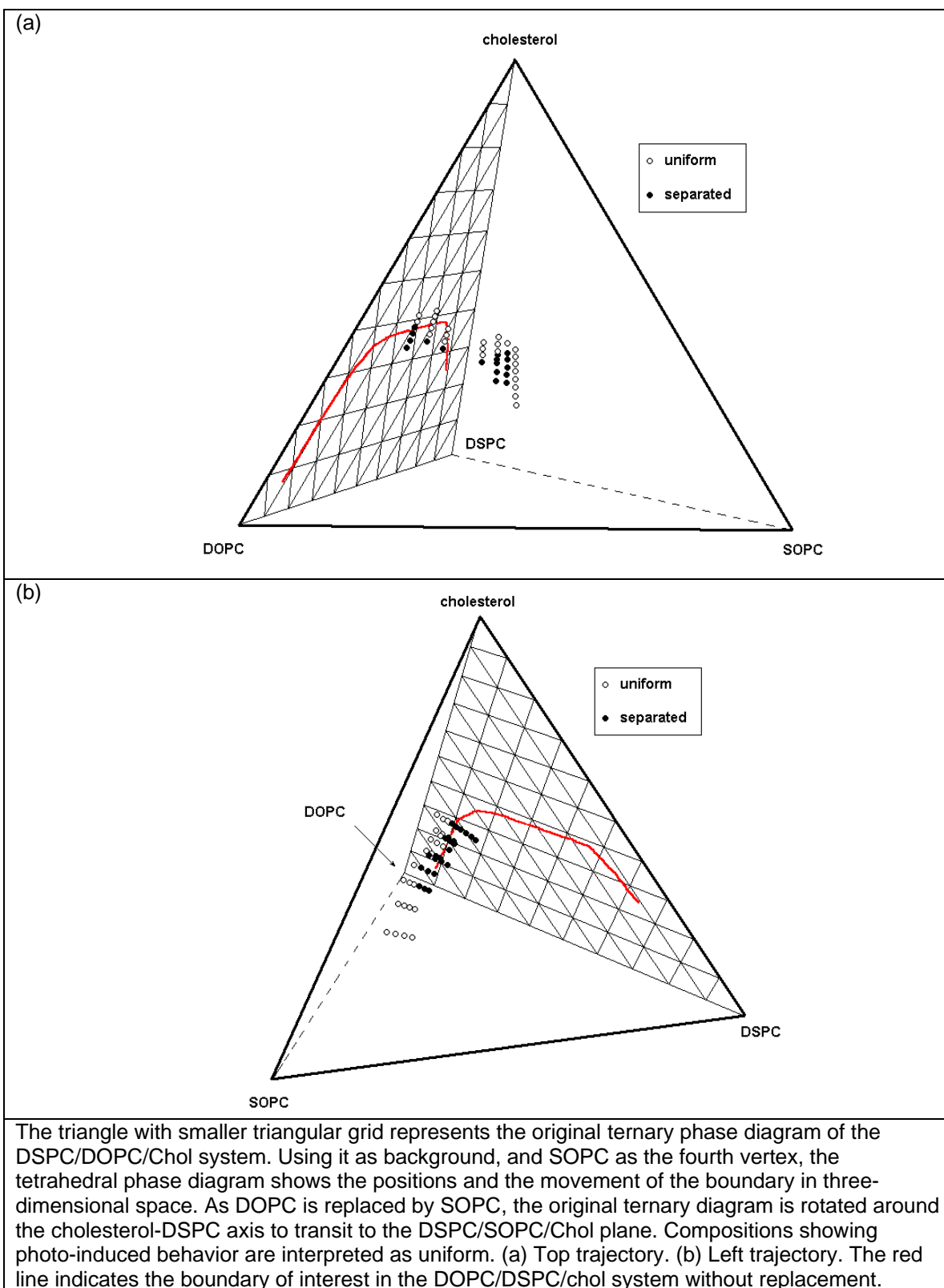
Specifically for the left trajectory in this experiment, C12:0-DiI partitions into the larger $L\alpha$ phase, therefore, it is possible that phase-separation of a small amount of L_o phase was mistakenly recognized as uniform, and the boundary position was mistakenly determined at a higher concentration of DSPC than it actually was. However, the direction and the extent of the boundary shift would be unaffected by the inability to detect small L_o phase, as long as a consistent judgment was used. Ideally, a fluorescent

dye that partitions into the Lo phase would be best for this region, such as C20:0-DiI (12, 13).

The Tetrahedral Phase Diagrams

Although far more data are needed to generate the complete three-dimensional tetrahedral phase diagram, it is still insightful to plot the available data points to examine the position and movement of the boundary in three-dimensional space (Figure 8, generated by Mathematica).

Figure 8 The Tetrahedral Phase Diagrams

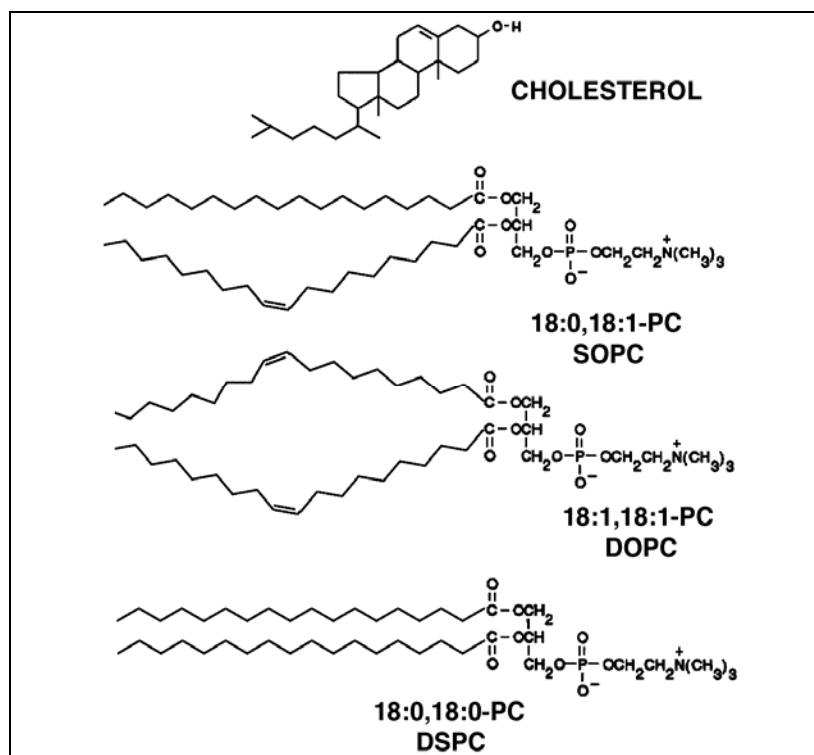


The Interactions and the Structures of the Lipids

The shrinkage of the two-phase region and the expansion of the one-phase region indicate higher miscibility of DSPC/SOPC/chol compared with DSPC/DOPC/chol. This result indicates more favorable interactions of SOPC with cholesterol and/or DSPC, compared with DOPC with cholesterol and/or DSPC. The interactions among the phospholipids can be explained by the structures of the phospholipids (Figure 9): DOPC, DSPC, and SOPC all have acyl chains of 18 carbons. However, DOPC has two unsaturated chains; DSPC has two saturated chains; and SOPC has one unsaturated and one saturated chains. Therefore, it is reasonable that SOPC mixes better with DSPC. The change of the phase regions could also be due to the more favorable interaction of SOPC with cholesterol, compared to DOPC with cholesterol. However, by the structures alone, the interactions between the phospholipids and cholesterol are not obvious.

If the fourth component introduced into the DSPC/DOPC/chol system, unlike SOPC, has poorer interactions with cholesterol and/or DSPC, the two-phase region is expected to expand. Whether the fourth component has more favorable or poorer interaction with cholesterol or DSPC should therefore be distinguishable.

Figure 9 Comparison of the Phospholipids Used in the Experiment



CONCLUSION

Although not very precise, the overall direction and extent of the boundary movement upon replacement of DOPC by SOPC were determined, and could be explained by the structures of the phospholipid components. Low percentage replacement of DOPC by SOPC shifts the middle part of the high cholesterol boundary of the $L\alpha + L_o$ two-phase region to a lower percentage of cholesterol, whereas higher percentage replacement brings about the photo-induced effects, which obscures the real phase behavior. The $L\alpha$ side of the boundary remains essentially unchanged below 50% replacement of DOPC by SOPC, and no phase-separation was found above 70% replacement. The success of this experiment proved the original DSPC/DOPC/chol system to be a powerful platform to study phase behaviors of other lipids.

As mentioned in the Discussion section, further studies are required to obtain a more accurate picture of all parts of the boundary. Besides, this project can also branch out in many directions. First, one more trajectory could be investigated on the Lo side of the boundary to obtain a more complete picture of the boundary shifts. Second, after the examination of SOPC, we can continue to study lipids with more unsaturated chains, such as 18:0-18:2 PC and 18:0-22:6 PC, as mentioned in the Introduction section. Third, the same set of methods can be used to study the effects of these lipids on other boundaries of the phase diagram. Also, one can investigate the nature and biological significance of the photo-induction phenomenon, starting by characterizing the properties of this phenomenon.

APPENDIX

Appendix A Results of Phase Behaviors

(a) Top Trajectory			(b) Left Trajectory		
DOPC Percentage Replaced by SOPC	Cholesterol Percentage	Phase Behaviors	DOPC Percentage Replaced by SOPC	DSPC Percentage	Phase Behaviors
0.0%	33.3%	s	0.0%	4.5%	u
	35.0%	s		6.6%	u
	36.6%	s		8.0%	u
	38.1%	s		8.6%	u
	39.5%	u		9.4%	s
	40.9%	u		10.5%	s
10.3%	35.0%	s		10.8%	s
	36.6%	u		12.2%	s
	38.1%	u		12.3%	s
	39.5%	u		14.1%	s
	40.9%	pi		15.8%	s
	42.2%	u		17.4%	s
20.6%	33.3%	s	10.3%	6.5%	u
	34.9%	pi		8.5%	u
	36.5%	u		10.5%	s
	38.0%	u		12.3%	s
43.7%	30.2%	s	12.4%	8.5%	u
	31.9%	pi		10.0%	s
	33.6%	pi		11.5%	s
	35.1%	u		12.9%	s
52.2%	25.9%	s	18.5%	6.6%	u
	28.0%	s		8.7%	u
	30.1%	s		10.6%	u
	31.1%	s		12.5%	s
	32.1%	s	27.0%	7.5%	u
	33.0%	pi		8.9%	u
	34.8%	pi		10.2%	s
	36.5%	pi		11.5%	s
58.0%	25.5%	s	28.9%	8.6%	s
	27.4%	s		10.6%	s
	29.3%	s		12.4%	s
	31.0%	s		14.2%	s
	32.7%	s	39.3%	6.6%	u
	35.1%	pi		8.6%	s
62.7%	20.1%	pi		10.6%	s
	22.3%	pi		12.4%	s
	24.4%	pi	51.8%	6.5%	u
	26.4%	pi		8.0%	u
	28.3%	pi		9.4%	u
	30.1%	pi		10.8%	s
	31.9%	pi		12.2%	s
	33.5%	pi		13.5%	s
88.3%				8.5%	u
			68.1%	10.0%	u
				11.5%	u
				12.9%	u
				9.9%	u
			88.3%	12.0%	u
				14.1%	u
				16.1%	u

Legend: s: separated. u: uniform. pi: photo-induced separated.

ACKNOWLEDGMENTS

This work was funded by US National Science Foundation Grant MCB-0315330, American Chemical Society Grant PRF-38464-AC7 to Gerald W. Feigenson, and supported by 2006 Cornell Hughes Scholar Program for the author.

The author thanks the primary investigator Gerald W. Feigenson for constant advices on all aspects of the project, Jiang Zhao, Jing Wu, Adam T. Hammond, Nelson F. Morales, Frederick A. Heberle, Thalia T. Mills for experimental technique training and Huilin Shao for insightful discussion.

REFERENCES

1. Singer, S. J. and G.L. Nicolson 1972. The fluid mosaic model of the structure of cell membranes. *Science*. 175, 720-731.
2. Simons, K. and E. Ikonen 1997. Functional rafts in cell membranes. *Nature*. 387, 569-572.
3. Rietveld, A. and K. Simons 1998. The differential miscibility of lipids as the basis for the formation of functional membrane rafts. *Biochim. Biophys. Acta*. 1376, 467-479.
4. Simons, K. and G. van Meer 1988. Lipid sorting in epithelial cells. *Biochemistry*. 27, 6197-6202.
5. Staneva, G., M.I. Angelova and K. Koumanov 2004. Phospholipase A2 promotes raft budding and fission from giant liposomes. *Chem. Phys. Lipids*. 129, 53-62.
6. Feigenson, G. W. 2006. Phase behavior of lipid mixtures. *Nat. Chem. Biol.* 2, 560-563.
7. Zachowski, A. 1993. Phospholipids in animal eukaryotic membranes: Transverse asymmetry and movement. *Biochem. J.* 294 (Pt 1), 1-14.
8. Lands, W. E. 1992. Biochemistry and physiology of n-3 fatty acids. *FASEB J.* 6, 2530-2536.
9. Kingsley, P. B. and G.W. Feigenson 1979. The synthesis of a perdeuterated phospholipid: 1,2-dimyristoyl-*sn*-glycero-3-phosphocholine- d_{72} . *Chem. Phys. Lipids*. 24, 135-147.
10. Angelova, M. I. and D.S. Dimitrov 1986. Liposome electroformation. *Faraday Discuss. Chem. Soc.* 81, 303-311.
11. Angelova, M. I., S. Soleau, P. Meleard, J.F. Faucon and P. Bothorel Preparation of giant vesicles by external AC electric fields. kinetics and applications. *Progr. Colloid Polym. Sci.* 89, 127-131.
12. Feigenson, G. W. and J.T. Buboltz 2001. Ternary phase diagram of dipalmitoyl-PC/dilauroyl-PC/cholesterol: Nanoscopic domain formation driven by cholesterol. *Biophys. J.* 80, 2775-2788.
13. Korlach, J., P. Schwille, W.W. Webb and G.W. Feigenson 1999. Characterization of lipid bilayer phases by confocal microscopy and fluorescence correlation spectroscopy. *Proc. Natl. Acad. Sci. U. S. A.* 96, 8461-8466.